

## Branching Fractions for $\psi(2S)$ -to- $J/\psi$ Transitions

N. E. Adam,<sup>1</sup> J. P. Alexander,<sup>1</sup> K. Berkelman,<sup>1</sup> D. G. Cassel,<sup>1</sup> V. Crede,<sup>1</sup> J. E. Duboscq,<sup>1</sup>  
K. M. Ecklund,<sup>1</sup> R. Ehrlich,<sup>1</sup> L. Fields,<sup>1</sup> R. S. Galik,<sup>1</sup> L. Gibbons,<sup>1</sup> B. Gittelman,<sup>1</sup>  
R. Gray,<sup>1</sup> S. W. Gray,<sup>1</sup> D. L. Hartill,<sup>1</sup> B. K. Heltsley,<sup>1</sup> D. Hertz,<sup>1</sup> L. Hsu,<sup>1</sup>  
C. D. Jones,<sup>1</sup> J. Kandaswamy,<sup>1</sup> D. L. Kreinick,<sup>1</sup> V. E. Kuznetsov,<sup>1</sup> H. Mahlke-Krüger,<sup>1</sup>  
T. O. Meyer,<sup>1</sup> P. U. E. Onyisi,<sup>1</sup> J. R. Patterson,<sup>1</sup> D. Peterson,<sup>1</sup> E. A. Phillips,<sup>1</sup>  
J. Pivarski,<sup>1</sup> D. Riley,<sup>1</sup> A. Ryd,<sup>1</sup> A. J. Sadoff,<sup>1</sup> H. Schwarthoff,<sup>1</sup> M. R. Shepherd,<sup>1</sup>  
S. Stroiney,<sup>1</sup> W. M. Sun,<sup>1</sup> D. Urner,<sup>1</sup> T. Wilksen,<sup>1</sup> M. Weinberger,<sup>1</sup> S. B. Athar,<sup>2</sup>  
P. Avery,<sup>2</sup> L. Brevina-Newell,<sup>2</sup> R. Patel,<sup>2</sup> V. Potlia,<sup>2</sup> H. Stoeck,<sup>2</sup> J. Yelton,<sup>2</sup> P. Rubin,<sup>3</sup>  
C. Cawfield,<sup>4</sup> B. I. Eisenstein,<sup>4</sup> G. D. Gollin,<sup>4</sup> I. Karliner,<sup>4</sup> D. Kim,<sup>4</sup> N. Lowrey,<sup>4</sup>  
P. Naik,<sup>4</sup> C. Sedlack,<sup>4</sup> M. Selen,<sup>4</sup> J. Williams,<sup>4</sup> J. Wiss,<sup>4</sup> K. W. Edwards,<sup>5</sup> D. Besson,<sup>6</sup>  
T. K. Pedlar,<sup>7</sup> D. Cronin-Hennessy,<sup>8</sup> K. Y. Gao,<sup>8</sup> D. T. Gong,<sup>8</sup> Y. Kubota,<sup>8</sup> T. Klein,<sup>8</sup>  
B. W. Lang,<sup>8</sup> S. Z. Li,<sup>8</sup> R. Poling,<sup>8</sup> A. W. Scott,<sup>8</sup> A. Smith,<sup>8</sup> S. Dobbs,<sup>9</sup> Z. Metreveli,<sup>9</sup>  
K. K. Seth,<sup>9</sup> A. Tomaradze,<sup>9</sup> P. Zweber,<sup>9</sup> J. Ernst,<sup>10</sup> A. H. Mahmood,<sup>10</sup> H. Severini,<sup>11</sup>  
D. M. Asner,<sup>12</sup> S. A. Dytman,<sup>12</sup> W. Love,<sup>12</sup> S. Mehrabyan,<sup>12</sup> J. A. Mueller,<sup>12</sup> V. Savinov,<sup>12</sup>  
Z. Li,<sup>13</sup> A. Lopez,<sup>13</sup> H. Mendez,<sup>13</sup> J. Ramirez,<sup>13</sup> G. S. Huang,<sup>14</sup> D. H. Miller,<sup>14</sup>  
V. Pavlunin,<sup>14</sup> B. Sanghi,<sup>14</sup> E. I. Shibata,<sup>14</sup> I. P. J. Shipsey,<sup>14</sup> G. S. Adams,<sup>15</sup>  
M. Chasse,<sup>15</sup> M. Cravey,<sup>15</sup> J. P. Cummings,<sup>15</sup> I. Danko,<sup>15</sup> J. Napolitano,<sup>15</sup> Q. He,<sup>16</sup>  
H. Muramatsu,<sup>16</sup> C. S. Park,<sup>16</sup> W. Park,<sup>16</sup> E. H. Thorndike,<sup>16</sup> T. E. Coan,<sup>17</sup> Y. S. Gao,<sup>17</sup>  
F. Liu,<sup>17</sup> M. Artuso,<sup>18</sup> C. Boulahouache,<sup>18</sup> S. Blusk,<sup>18</sup> J. Butt,<sup>18</sup> E. Dambasuren,<sup>18</sup>  
O. Dorjkhaidav,<sup>18</sup> J. Li,<sup>18</sup> N. Mena,<sup>18</sup> R. Mountain,<sup>18</sup> R. Nandakumar,<sup>18</sup> R. Redjimi,<sup>18</sup>  
R. Sia,<sup>18</sup> T. Skwarnicki,<sup>18</sup> S. Stone,<sup>18</sup> J. C. Wang,<sup>18</sup> K. Zhang,<sup>18</sup> S. E. Csorna,<sup>19</sup>  
G. Bonvicini,<sup>20</sup> D. Cinabro,<sup>20</sup> M. Dubrovin,<sup>20</sup> R. A. Briere,<sup>21</sup> G. P. Chen,<sup>21</sup> J. Chen,<sup>21</sup>  
T. Ferguson,<sup>21</sup> G. Tatishvili,<sup>21</sup> H. Vogel,<sup>21</sup> M. E. Watkins,<sup>21</sup> and J. L. Rosner<sup>22</sup>

(CLEO Collaboration)

<sup>1</sup>Cornell University, Ithaca, New York 14853

<sup>2</sup>University of Florida, Gainesville, Florida 32611

<sup>3</sup>George Mason University, Fairfax, Virginia 22030

<sup>4</sup>University of Illinois, Urbana-Champaign, Illinois 61801

<sup>5</sup>Carleton University, Ottawa, Ontario, Canada K1S 5B6  
and the Institute of Particle Physics, Canada

<sup>6</sup>University of Kansas, Lawrence, Kansas 66045

<sup>7</sup>Luther College, Decorah, Iowa 52101

<sup>8</sup>University of Minnesota, Minneapolis, Minnesota 55455

<sup>9</sup>Northwestern University, Evanston, Illinois 60208

<sup>10</sup>State University of New York at Albany, Albany, New York 12222

<sup>11</sup>University of Oklahoma, Norman, Oklahoma 73019

<sup>12</sup>University of Pittsburgh, Pittsburgh, Pennsylvania 15260

<sup>13</sup>University of Puerto Rico, Mayaguez, Puerto Rico 00681

<sup>14</sup>Purdue University, West Lafayette, Indiana 47907

<sup>15</sup>Rensselaer Polytechnic Institute, Troy, New York 12180

<sup>16</sup>University of Rochester, Rochester, New York 14627

<sup>17</sup>Southern Methodist University, Dallas, Texas 75275

<sup>18</sup>Syracuse University, Syracuse, New York 13244

<sup>19</sup>Vanderbilt University, Nashville, Tennessee 37235

<sup>20</sup>Wayne State University, Detroit, Michigan 48202

<sup>21</sup>Carnegie Mellon University, Pittsburgh, Pennsylvania 15213

<sup>22</sup>Enrico Fermi Institute, University of Chicago, Chicago, Illinois 60637

(Dated: March 16, 2005)

## Abstract

We describe new measurements of the inclusive and exclusive branching fractions for  $\psi(2S)$  transitions to  $J/\psi$  using  $e^+e^-$  collision data collected with the CLEO detector operating at CESR. All branching fractions and ratios of branching fractions reported here represent either the most precise measurements to date or the first direct measurements. Indirectly and in combination with other CLEO measurements, we determine  $\mathcal{B}(\chi_{cJ} \rightarrow \gamma J/\psi)$  and  $\mathcal{B}[\psi(2S) \rightarrow \text{light hadrons}]$ .

Heavy quarkonium states, non-relativistic bound  $c\bar{c}$  or  $b\bar{b}$  systems, offer a laboratory to study the strong interaction in the non-perturbative regime. Charmonium in particular has served as a calibration tool for the corresponding techniques and models [1]. The experimental situation for  $\psi(2S)$  decays has only begun to approach precisions at the percent level, with a global fit to the myriad of measurements from different experiments and eras revealing possible systematic inconsistencies [2]. Clarification of this picture is warranted.

This Letter presents branching fraction measurements of the four exclusive hadronic transitions  $\psi(2S) \rightarrow J/\psi + h$  ( $h = \pi^+\pi^-, \pi^0\pi^0, \eta, \pi^0$ ), the exclusive channels  $\psi(2S) \rightarrow J/\psi + \gamma\gamma$  through  $\psi(2S) \rightarrow \gamma\chi_{cJ}$ , an inclusive measurement of  $\psi(2S) \rightarrow XJ/\psi$ , ratios between the above, and several derived quantities. Multiple issues can be investigated with this data: the observed discrepancy [3] between  $\mathcal{B}(\pi^0\pi^0 J/\psi)/\mathcal{B}(\pi^+\pi^- J/\psi)$  and the isospin-based expectation awaits corroboration;  $\pi^0 J/\psi$  as an isospin-violating decay, when compared with  $\eta J/\psi$ , helps constrain quark mass ratios [4]; the  $\chi_{cJ}$  data offer access to the  $\chi_{cJ} \rightarrow \gamma J/\psi$  rates in combination with the  $\psi(2S) \rightarrow \gamma\chi_{cJ}$  branching fractions [5]; confirmation of the transition  $\psi(2S) \rightarrow \gamma\chi_{c0} \rightarrow \gamma\gamma J/\psi$  [6, 7]; and the first direct constraint of  $\mathcal{B}(\psi(2S) \rightarrow \text{light hadrons})$  using measurements from only one experiment.

We use  $e^+e^-$  collision data at and below the  $\psi(2S)$  resonance,  $\sqrt{s} = 3.686$  GeV ( $\mathcal{L} = 5.86$  pb $^{-1}$ ) and  $\sqrt{s} = 3.670$  GeV (“continuum” data,  $\mathcal{L} = 20.46$  pb $^{-1}$ ), collected with the CLEO detector [8] operating at the Cornell Electron Storage Ring (CESR) [9]. The detector features a solid angle coverage of 93% for charged and neutral particles. The charged particle tracking system operates in a 1.0 T magnetic field along the beam axis and achieves a momentum resolution of  $\sim 0.6\%$  at momenta of 1 GeV/ $c$ . The CsI crystal calorimeter attains photon energy resolutions of 2.2% for  $E_\gamma = 1$  GeV and 5% at 100 MeV.

The  $J/\psi$  is identified through its decay to  $\mu^+\mu^-$  or  $e^+e^-$ , and we demand that  $m(J/\psi) \equiv m(\ell^+\ell^-) = 3.02 - 3.22$  GeV. The ratios of calorimeter shower energy to track momentum,  $E/p$ , for the lepton candidates, taken to be the two tracks of highest momentum in the event, must be larger than 0.85 for one electron and above 0.5 for the other, or smaller than 0.25 and below 0.5 for muon pairs. In order to salvage lepton pairs that have radiated photons and would hence fail the  $m(J/\psi)$  cut, we add bremsstrahlung photon candidates found within a cone of 100 mrad to the three-vector of each lepton track at the interaction point (IP). For  $\psi(2S) \rightarrow XJ/\psi$ , cosmic ray background is rejected based on the distance of the track impact parameters to the IP ( $< 2$  mm), and on the  $J/\psi$  momentum ( $p_{J/\psi} > 50$  MeV/ $c$ ). Radiative lepton pair production and radiative returns to the  $J/\psi$  are suppressed for this mode by demanding  $|\cos\theta_{J/\psi}| < 0.98$ .

For the exclusive final states, requirements on momentum and energy conservation are imposed:  $(E_{J/\psi} + E_X)/\sqrt{s} = 0.95 - 1.05$ ,  $||p_{J/\psi}| - |p_X||/\sqrt{s} < 0.07$ . For  $\eta$  and single- $\pi^0$  transitions, in which the  $J/\psi$  is monochromatic,  $p(J/\psi)$  must lie within 500 – 570 MeV/ $c$  ( $\pi^0$ ) or 150 – 250 MeV/ $c$  ( $\eta$ ). Charged dipion transition candidates must have two tracks of opposite charge lower in momentum than the lepton pair. We identify neutral pions through their decay into two photons. Photon candidates must not align with the projection of any track into the calorimeter. We require  $m(\gamma\gamma) = 90 - 170$  MeV for  $\pi^0$  mesons in  $\pi^0\pi^0 J/\psi$  and  $\eta \rightarrow \pi^+\pi^-\pi^0$ ; stricter conditions are imposed in  $\pi^0 J/\psi$  to suppress background from  $\psi(2S) \rightarrow J/\psi\gamma\gamma$  through  $\chi_{cJ}$ :  $m(\gamma\gamma) = 110 - 150$  MeV, and in addition a constraint that the decay not be too asymmetric. We find  $\eta$  meson candidates through  $\eta \rightarrow \gamma\gamma$  or  $\eta \rightarrow \pi^+\pi^-\pi^0$  with  $m(\gamma\gamma)$  or  $m(\pi^+\pi^-\pi^0) = 500 - 580$  MeV. The  $\pi^+\pi^-e^+e^-$  final state must have  $m(\pi^+\pi^-) > 350$  MeV to suppress background from radiative Bhabha events with subsequent  $\gamma \rightarrow e^+e^-$  conversion. The invariant mass of the system recoiling against

the  $\pi^+\pi^-$  or  $\pi^0\pi^0$  must lie inside 3.05 – 3.15 GeV. To reduce background from radiative transitions to  $\chi_{c1,2}$  into  $\pi^0 J/\psi$  and  $\eta(\rightarrow \gamma\gamma)J/\psi$ , the least energetic photon in the  $\eta$  or  $\pi^0$  candidate has to fulfill  $E_\gamma > 200$  MeV;  $E_\gamma = 30 - 100$  MeV is also allowed for the  $\pi^0$  in  $\pi^0 J/\psi$ . In general, photons must have  $|\cos\theta_\gamma|_{\max} < 0.93$ ; for  $\pi^0 J/\psi$ , we require  $|\cos\theta_\gamma|_{\max} < 0.8$  to suppress radiative lepton pair background with a fake  $\pi^0$ . Candidates for  $\gamma\chi_{cJ} \rightarrow \gamma\gamma J/\psi$  are accepted if  $p_{J/\psi} = 250 - 500$  MeV (to suppress background from  $\pi^0, \eta J/\psi$ ), the recoil mass from the two photons is within 3.05 – 3.13 GeV, and the energy of the second most energetic photon,  $E_{\gamma\text{-low}}$ , is within 90 – 150, 145 – 200, and 230 – 290 MeV ( $J = 2, 1$ , and 0).

Table I displays for each mode the raw event counts obtained with this selection as well as the efficiency  $\epsilon$ , which is determined from Monte Carlo (MC) simulation using the `EvtGen` generator [10] and a GEANT-based [11] detector simulation together with corrections based on the data. The dipion invariant mass distribution as produced by `EvtGen` is slightly suppressed at high and low  $m(\pi\pi)$  to better match the data, altering the efficiencies by  $< 0.5\%$ . The  $\chi_{cJ}$  MC samples use intrinsic widths from Ref. [2], and angular distributions have been generated according to the prescription in Ref. [12]. The  $XJ/\psi$  data sample is modeled by the sum of all exclusive MC channels, weighted by their measured branching fractions. The trigger efficiencies for all modes are measured using a prescaled subset of candidates in each channel that fulfilled much looser requirements.

Data distributions of representative variables are shown in Figures 1-4 and compared to MC predictions. All figures show distributions in which all selection criteria have been applied to all variables *except* for the one shown. The MC predictions in all figures depict the sum of all exclusive channels; each source has been normalized to our final branching fractions. Distributions of invariant masses, angles, and momenta show excellent agreement between MC and data for all channels.

The observed event rates on the  $\psi(2S)$  are corrected for contributions from continuum production and  $\psi(2S)$  cross-feed. In all  $\mu^+\mu^-$  and most  $e^+e^-$  modes, the observed continuum yield is attributable to the Breit-Wigner tail of the  $\psi(2S)$ . The only significant  $\psi(2S)$ -induced backgrounds stem from cross-feed between the signal modes and from  $J/\psi \rightarrow \pi^+\pi^-$  and  $\rho\pi$ . We estimate the sum of all contributions to each channel from MC simulation by determining for each signal MC what fraction passes the selection criteria of all other channels relative to its own detection efficiency. Cross-feed subtraction does not result in a significant reduction of the event yield for most channels (see Table I). When analysis techniques similar to those in Refs. [6, 7] are applied to final states consisting of a  $J/\psi$  and two photons, yields consistent with those presented here are obtained.

In order to measure the  $\pi^\pm, \pi^0$ , and lepton detection efficiencies, we study  $\psi(2S) \rightarrow \pi\pi J/\psi, J/\psi \rightarrow \ell^+\ell^-$  decays in which the selection of one pion (neutral or charged) or lepton is replaced by kinematic restrictions. The samples thus obtained are very clean and give direct access to the reconstruction efficiency of the not explicitly required, but usually present, particle. We correct predicted MC efficiencies with the observed, small MC-data discrepancies (all  $\sim 1\%$  or less) found in these studies and include them in the efficiencies in Table I. In the case of the dilepton selections, these corrections absorb both any detector mismodeling and also that of decay radiation [13]. Relative systematic errors from these studies are 0.75% for each photon pair, 0.4% per  $\pi^\pm$ , 0.5% per  $\mu^+\mu^-$ , and 0.2% per  $e^+e^-$ . The uncertainty of lepton pair identification efficiency is 0.1%.

The systematic uncertainty stemming from cross-feed and background subtraction is a small contribution to the total error, with the exception of  $\pi^0 J/\psi$  (2.4%). To account

for potential mismodeling of the two-photon recoil mass distribution, the  $\gamma\gamma J/\psi$  channels are assigned an additional 2% uncertainty. In the energy distribution of the second-most energetic photon in  $\gamma\chi_{cJ} \rightarrow \gamma\gamma J/\psi$  candidates, the data show an unexpected population in the region between the  $\chi_{c1}$  and  $\chi_{c0}$  (Figure 4). The events in  $E_{\gamma\text{-low}} = 200 - 230$  MeV do not show any firm evidence for significant contamination from continuum ( $e^+e^-$  annihilation not through a  $\psi(2S)$ ), non- $J/\psi$  backgrounds, anomalous levels of  $\pi^0 J/\psi$  or  $\eta J/\psi$ , or an unmodeled, anomalously broad photon energy resolution, although small fluctuations in all the sources mentioned are possible. We cannot exclude that these events originate at least partially from a high-side tail of the  $\gamma\chi_{c1}$  cascades not modeled by MC, or as non-resonant  $\gamma\gamma J/\psi$ , or that  $\Gamma(\chi_{c0}) = 10.1$  MeV [2] is an underestimate. As no single source can be isolated and hence the continuation of the background shape under the  $\chi_{c0}$  peak is unknown, we apply an additional 10% uncertainty for the  $\chi_{c0}$  mode. We add the above, the uncertainty on the  $J/\psi \rightarrow \ell^+\ell^-$  branching fraction (1.2% [14]), and 3% as the estimate of the precision of the number of  $\psi(2S)$  decays [5], all in quadrature. This last contribution dominates the systematic error in the absolute branching fractions, with the exception of  $\gamma\chi_{c0} \rightarrow \gamma\gamma J/\psi$ . Correlations between errors have been taken into account when combining  $e^+e^-$  and  $\mu^+\mu^-$  subsamples. Many systematic uncertainties cancel in the ratios.

The branching fractions are readily obtained from the raw event yield after background subtraction and correction for efficiency by dividing by the number of  $\psi(2S)$  decays,  $3.08 \times 10^6$ , estimated by the method described in Ref. [5], and the  $J/\psi \rightarrow \ell^+\ell^-$  branching fraction,  $(5.953 \pm 0.056 \pm 0.042)\%$  [14]. We also compute branching fraction ratios between  $XJ/\psi$  and all exclusive modes and as well as  $\pi^+\pi^- J/\psi$  and all other exclusive modes. These results are included in Table I.

Our investigation of the  $J/\psi + h$  branching fractions yields broad agreement with previous results. The  $\pi^0\pi^0 J/\psi$  and  $\eta(\rightarrow \pi^+\pi^-\pi^0) J/\psi$  measurements, along with many of the ratios of branching fractions, are firsts of their kind. The total errors match or improve upon current best measurements [2, 3]. We observe the  $\psi(2S) \rightarrow \gamma\chi_{cJ} \rightarrow \gamma\gamma J/\psi$  branching fractions to be slightly larger than BES [7] and much larger than CBAL [6], but the excellent agreement between our exclusive branching fraction sum and the inclusive  $J/\psi$  rate reinforces the accuracy and internal consistency of this work. We obtain  $\Sigma\mathcal{B}[\psi(2S) \rightarrow J/\psi + h] + \Sigma\mathcal{B}(\psi(2S) \rightarrow \gamma\chi_{cJ} \rightarrow \gamma\gamma J/\psi) = (58.9 \pm 0.2 \pm 2.0)\%$ , consistent with  $\mathcal{B}(\psi(2S) \rightarrow XJ/\psi)$ , thereby not leaving much room,  $(0.6 \pm 0.4)\%$ , for other transitions to the  $J/\psi$ . The branching fractions for transitions through the  $h_c$ ,  $\psi(2S) \rightarrow \gamma\eta_c(2S) \rightarrow \gamma\gamma J/\psi$ , and  $\psi(2S) \rightarrow \gamma\gamma J/\psi$  as a direct process are not expected to exceed the observed difference.

These results enable us to calculate several derived quantities. We measure the neutral and charged dipion branching fraction to be consistent with the isospin-based expectation of 1:2. The branching fraction for  $\psi(2S)$  decaying to light hadrons, computed as the difference between unity and the branching fraction sum of all exclusive direct transitions measured in this work ( $\Sigma\mathcal{B}[\psi(2S) \rightarrow J/\psi + h] = (53.4 \pm 0.2 \pm 1.7)\%$ ), the radiative decays [ $\psi(2S) \rightarrow \chi_{cJ}\gamma$  and  $\psi(2S) \rightarrow \gamma\eta_c$ , and the dilepton branching fractions [2], is found to be  $\mathcal{B}[\psi(2S) \rightarrow \text{light hadrons}] = (16.9 \pm 2.6)\%$ . It can be compared with that of the  $J/\psi$ ,  $\mathcal{B}(J/\psi \rightarrow \text{light hadrons}) = (86.8 \pm 0.4)\%$  [2, 14], yielding a ratio of  $(19.4 \pm 3.0)\%$ . Applying the “12% rule” [15] to inclusive decays [16], the ratio is  $\sim 2.2\sigma$  above  $\mathcal{B}[\psi(2S) \rightarrow \ell^+\ell^-]/\mathcal{B}(J/\psi \rightarrow \ell^+\ell^-) = (12.6 \pm 0.7)\%$  [2, 14]. Combining the doubly-radiative branching fractions analyzed in this study with those for  $\psi(2S) \rightarrow \gamma\chi_{cJ}$  [5], we arrive at  $\mathcal{B}(\chi_{c0} \rightarrow \gamma J/\psi) = (2.0 \pm 0.2 \pm 0.2)\%$ ,  $\mathcal{B}(\chi_{c1} \rightarrow \gamma J/\psi) = (37.9 \pm 0.8 \pm 2.1)\%$ , and  $\mathcal{B}(\chi_{c2} \rightarrow \gamma J/\psi) = (19.9 \pm 0.5 \pm 1.2)\%$ , significantly higher than previous measurements for  $J = 0, 1$ . We measure the branching

fraction ratio  $\mathcal{B}[\psi(2S) \rightarrow \pi^0 J/\psi]/\mathcal{B}[\psi(2S) \rightarrow \eta J/\psi] = (4.1 \pm 0.4 \pm 0.1)\%$ , to be compared with predictions ranging from 1.6% ([7] based on Ref. [17]) to 3.4% [4].

In summary, we have determined the branching fractions for all exclusive  $\psi(2S) \rightarrow J/\psi + h$  ( $h = \pi^+\pi^-, \pi^0\pi^0, \eta, \pi^0$ ) and  $\psi(2S) \rightarrow \gamma\chi_{cJ} \rightarrow \gamma\gamma J/\psi$  transitions, with a similar strategy applied to all channels. We obtain results for  $\mathcal{B}[\psi(2S) \rightarrow J/\psi + h]$  that are consistent with but more precise than previous measurements, where available, and  $\mathcal{B}[\psi(2S) \rightarrow \gamma\chi_{cJ} \rightarrow \gamma\gamma J/\psi]$  values both larger and more precise than previous measurements. The analysis is complemented by a study of the inclusive mode  $\psi(2S) \rightarrow XJ/\psi$ , the production rate of which is seen to be consistent with that of the sum of all expected exclusive contributions. Ratios between the branching fractions as well as results on  $\mathcal{B}(\chi_{cJ} \rightarrow \gamma J/\psi)$  are also tendered.

We gratefully acknowledge the effort of the CESR staff in providing us with excellent luminosity and running conditions. This work was supported by the National Science Foundation and the U.S. Department of Energy.

- 
- [1] N. Brambilla *et al.*, hep-ph/0412158, D. Besson, T. Skwarnicki, Ann. Rev. Nucl. Part. Sci. **43**, 333 (1993).
  - [2] S. Eidelman *et al.*, Phys. Lett. B Vol. 1 **592**, 1 (2004).
  - [3] BES Collaboration, M. Ablikim *et al.*, Phys. Rev. D **70**, 012003 (2004); E835 Collaboration, M. Andreotti *et al.*, Phys. Rev. D **71**, 032006 (2005).
  - [4] B.L. Ioffe, M.A. Shifman, Phys. Lett. B **95**, 99 (1980); B.L. Ioffe, M.A. Shifman, Phys. Lett. B **107**, 371 (1981); Y.-P. Kuang, S.F. Tuan, T.-M. Yan, Phys. Rev. D **37**, 1210 (1988).
  - [5] CLEO Collaboration, S.B. Athar *et al.*, Phys. Rev. D **70**, 112002 (2004).
  - [6] M. Oreglia *et al.*, Phys. Rev. D **25**, 2259 (1982).
  - [7] BES Collaboration, J.Z. Bai *et al.*, Phys. Rev. D **70**, 012006 (2004).
  - [8] CLEO Collaboration, Y. Kubota *et al.*, Nucl. Instrum. Methods Phys. Res., Sect. A **320**, 66 (1992); D. Peterson *et al.*, Nucl. Instrum. Methods Phys. Res., Sect. A **478**, 142 (2002); M. Artuso *et al.*, Nucl. Instrum. Methods Phys. Res., Sect. A **502**, 91 (2003).
  - [9] CLEO-c/CESR-c Taskforces & CLEO-c Collaboration, Cornell University LEPP Report No. CLNS 01/1742 (2001), unpublished.
  - [10] D.J. Lange, Nucl. Instrum. Methods Phys. Res., Sect. A **462**, 152 (2001).
  - [11] R. Brun *et al.*, GEANT 3.21, CERN Program Library Long Writeup W5013 (1993), unpublished.
  - [12] L.S. Brown and R.N. Cahn, Phys. Rev. D **13**, 1195 (1976).
  - [13] E. Barberio and Z. Was, Comput. Phys. Commun. **79**, 291 (1994).
  - [14] CLEO Collaboration, Z. Li *et al.*, Phys. Rev. D **71**, 111103(R) (2005).
  - [15] BES Collaboration, J.Z. Bai *et al.*, Phys. Rev. D **67**, 052002 (2003); *ibid.* **69**, 072001 (2004); CLEO Collaboration, S.B. Athar *et al.*, Phys. Rev. Lett. **94**, 012005 (2005) and references therein.
  - [16] Y.F. Gu and X.H. Li, Phys. Rev. D **63**, 114019 (2001).
  - [17] G.A. Miller, B.M.K. Nefkens, I. Slaus, Phys. Rept. **194**, 1 (1990).

TABLE I: For each mode: The detection efficiency,  $\epsilon$ , in percent; the numbers of events found in the  $\psi(2S)$  and continuum samples,  $N_{\psi(2S)}$  and  $N_{\text{cont}}$ ; the number of  $\psi(2S)$  related background events,  $N_{\text{bgd}}$ ; the branching fraction in percent and its ratio to  $\mathcal{B}_{\chi_{cJ}/\psi}$  and  $\mathcal{B}_{\pi^+\pi^-J/\psi}$ , also in percent.

Channel	$\epsilon$	$N_{\psi(2S)}$	$N_{\text{cont}}$	$N_{\text{bgd}}$	$\mathcal{B}$	$\mathcal{B}/\mathcal{B}_{\chi_{cJ}/\psi}$	$\mathcal{B}/\mathcal{B}_{\pi^+\pi^-J/\psi}$
$\pi^+\pi^-J/\psi$	49.3	60344	221	113	$33.54 \pm 0.14 \pm 1.10$	$56.37 \pm 0.27 \pm 0.46$	
$\pi^0\pi^0J/\psi$	22.2	13399	67	115	$16.52 \pm 0.14 \pm 0.58$	$27.76 \pm 0.25 \pm 0.43$	$49.24 \pm 0.47 \pm 0.86$
$\eta J/\psi$	22.6	2793	17	116	$3.25 \pm 0.06 \pm 0.11$	$5.46 \pm 0.10 \pm 0.07$	$9.68 \pm 0.19 \pm 0.13$
$\eta(\rightarrow \gamma\gamma)J/\psi$	16.9	2065	14	103	$3.21 \pm 0.07 \pm 0.11$	$5.39 \pm 0.12 \pm 0.06$	$9.56 \pm 0.21 \pm 0.14$
$\eta(\rightarrow \pi^+\pi^-\pi^0)J/\psi$	5.8	728	3	13	$3.39 \pm 0.13 \pm 0.13$	$5.70 \pm 0.21 \pm 0.13$	$10.10 \pm 0.38 \pm 0.22$
$\pi^0J/\psi$	13.9	88	3	20	$0.13 \pm 0.01 \pm 0.01$	$0.22 \pm 0.02 \pm 0.01$	$0.39 \pm 0.04 \pm 0.01$
$\gamma\chi_{c0} \rightarrow \gamma\gamma J/\psi$	23.4	172	20	17	$0.18 \pm 0.01 \pm 0.02$	$0.31 \pm 0.02 \pm 0.03$	$0.55 \pm 0.04 \pm 0.06$
$\gamma\chi_{c1} \rightarrow \gamma\gamma J/\psi$	30.6	3688	46	21	$3.44 \pm 0.06 \pm 0.13$	$5.77 \pm 0.10 \pm 0.12$	$10.24 \pm 0.17 \pm 0.23$
$\gamma\chi_{c2} \rightarrow \gamma\gamma J/\psi$	28.6	1915	56	62	$1.85 \pm 0.04 \pm 0.07$	$3.11 \pm 0.07 \pm 0.07$	$5.52 \pm 0.13 \pm 0.13$
$XJ/\psi$	65.3	151138	37916	123	$59.50 \pm 0.15 \pm 1.90$		

FIG. 1: For inclusively selected dimuon (left) and dielectron (right) events, the distributions of the dilepton mass in the  $\psi(2S)$  data (solid circles), after subtraction of the luminosity-scaled continuum, and in MC (solid line). The two peaks above 3.2 GeV in the  $m(\mu^+\mu^-)$  distributions correspond to backgrounds from  $\chi_{c0,2} \rightarrow K^+K^-$  and  $\chi_{c0} \rightarrow \pi^+\pi^-$ .

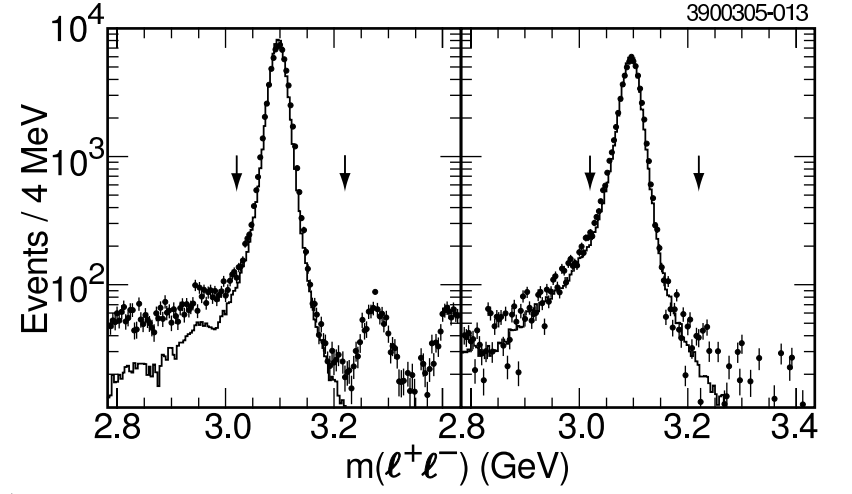


FIG. 2: For  $\psi(2S) \rightarrow \pi^+\pi^-\ell^+\ell^-$  (left) and  $\psi(2S) \rightarrow \pi^0\pi^0\ell^+\ell^-$  (right),  $e^+e^-$  and  $\mu^+\mu^-$  samples combined, candidate events in the  $\psi(2S)$  data (solid circles), MC simulation of signal (solid line), and  $\psi(2S) \rightarrow \eta J/\psi$  background (dashed histogram): distributions of the dilepton mass (top), the mass recoiling against the dipion pair (middle), and the invariant mass of the two pions.

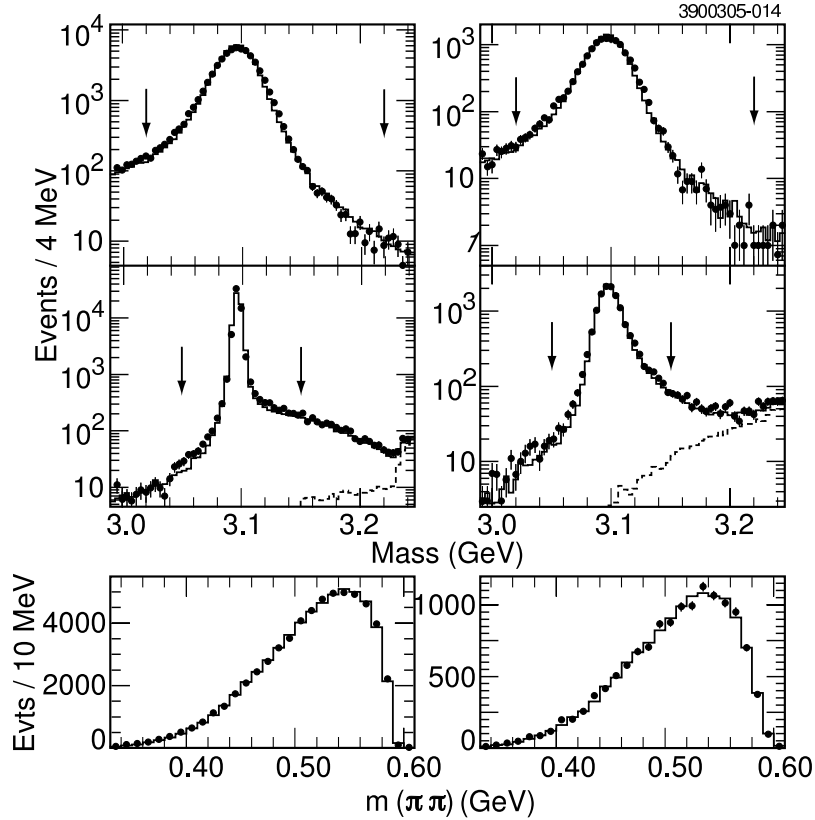


FIG. 3: For  $\psi(2S) \rightarrow \eta(\rightarrow \gamma\gamma, \pi^+\pi^-\pi^0)\ell^+\ell^-$  (left) and  $\psi(2S) \rightarrow \pi^0\ell^+\ell^-$  (right),  $e^+e^-$  and  $\mu^+\mu^-$  samples combined, candidate events in the  $\psi(2S)$  data (solid circles) and MC simulation of signal (solid line): distributions of the dilepton mass (top), the  $J/\psi$  momentum (middle), and the invariant mass of the two photons. In the lower left mass plot, the solid circles (data) and solid line (MC) apply to  $\eta \rightarrow \gamma\gamma$  decays, and the open circles (data) and the dashed histogram (MC) to  $\eta \rightarrow \pi^+\pi^-\pi^0$ .

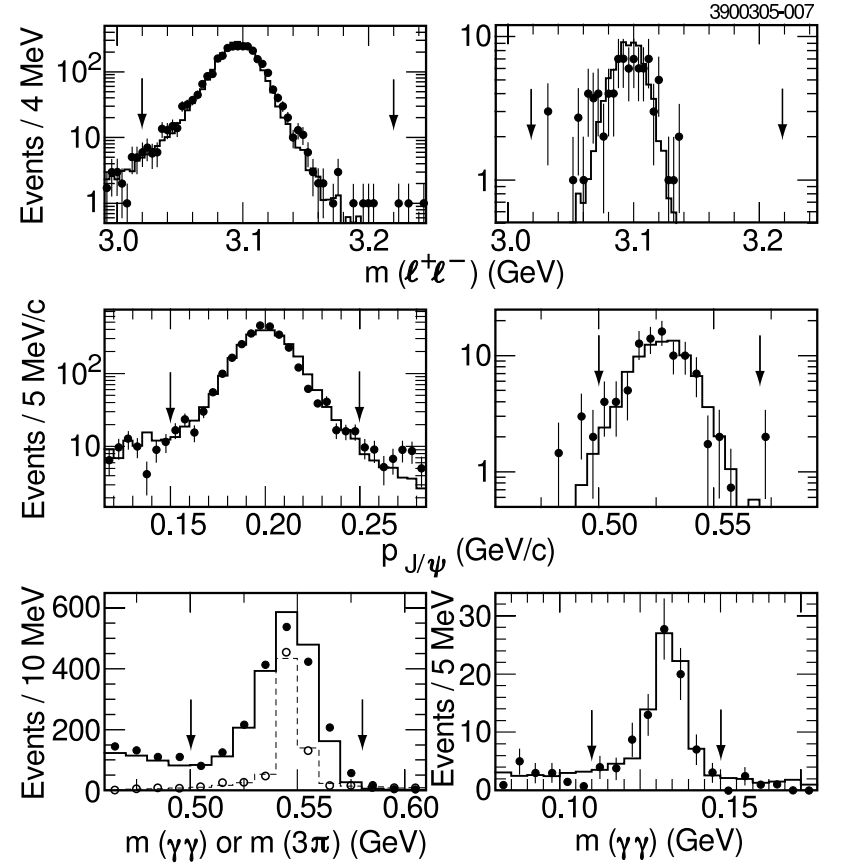


FIG. 4: For  $\psi(2S) \rightarrow \gamma\chi_{cJ}, \chi_{cJ} \rightarrow \gamma J/\psi, J/\psi \rightarrow \ell^+\ell^-$  candidate events in the  $\psi(2S)$  data (solid circles) and MC simulation of signal (solid line), the distribution of the energy of the second most energetic photon,  $E_{\gamma\text{-low}}$ , (top), and the two-photon recoil mass (bottom). The arrows indicate nominal cut values. The inset offers a close-up of the  $\chi_{c0}$  region. The broken lines represent  $\pi^0\pi^0 J/\psi$  MC.

